Published in final edited form as:
Exp Brain Res. 2008 August ; 189(4): 485–496. doi:10.1007/s00221-008-1444-3.

The Feedback Circuit Connecting the Central Mesencephalic Reticular Formation and the Superior Colliculus in the Macaque Monkey: Tectal Connections

Lan Zhou[1], **Susan Warren**[1], and **Paul J. May**[1,2,3]

[1] Department of Anatomy, University of Mississippi Medical Center, Jackson, MS 39216 U.S.A

[2] Department of Ophthalmology, University of Mississippi Medical Center, Jackson, MS 39216 U.S.A

[3] Department of Neurology, University of Mississippi Medical Center, Jackson, MS 39216 U.S.A

Abstract

The connectional and physiological characteristics of the central mesencephalic reticular formation (cMRF) indicate that it participates in gaze control. The cMRF receives projections from the ipsilateral superior colliculus (SC) via collaterals of predorsal bundle axons. These collaterals target cMRF neurons, which in turn project back upon the SC. In the present study, we examined the pattern of connections made by the cMRF reticulotectal projection by injecting the bidirectional neuroanatomical tracer, biotinylated dextran amine (BDA), into the cMRF of macaque monkeys. Anterogradely labeled reticulotectal terminals were found bilaterally in the SC, with an ipsilateral predominance, and were concentrated in the intermediate gray layer (SGI). BDA also retrogradely labeled SC neurons projecting to the cMRF. These labeled tectoreticular cells were located mainly in SGI. Injection site specific differences in the SC labeling pattern were evident, suggesting the lateral cMRF is more heavily connected to the upper sublamina of SGI, whereas the medial cMRF is more heavily connected with the lower sublamina. In view of the known downstream connections of the cMRF and these SC sublaminae, this organization intimates that the cMRF may contain subdivisions specialized to modulate the eye and the head components of gaze changes. In addition, reticulotectal terminals were observed to have close associations with retrogradely labeled tectoreticular cells in the ipsilateral SC, indicating possible synaptic contacts. Thus, the cMRF's reciprocal connections with the SC suggest this structure plays a role in defining the gaze-related bursting behavior of collicular output neurons.

Keywords

oculomotor; gaze; saccade; head movement

Introduction

The superior colliculus (SC) contains a map of contralaterally-directed gaze shifts, as indicated by studies in which electrical stimulation produced locus dependent saccade-like eye movements and related head turns, and by recording studies in which a burst of action potentials is present in SC neurons before gaze changes with a specific movement vector (Wurtz and Goldberg, 1972; Stryker and Schiller, 1975; Cowie and Robinson, 1994;

Send Correspondence To: Paul J. May, PhD, Department of Anatomy, University of Mississippi Medical Center, 2500 North State Street, Jackson, MS 39216, Phone# 601-984-1662, Fax# 601-984-1655, pmay@anatomy.umsmed.edu.

Freedman and Sparks, 1997). How the spatially coded signals found in the SC are formed, and exactly how they are transformed into firing appropriate to drive motoneurons remain open questions (Moschovakis et al., 1998). One structure that has been implicated in both the initial formation of the collicular signal and its spatiotemporal transformation is the central mesencephalic reticular formation (cMRF) (Cromer and Waitzman, 2006).

The cMRF was first defined by electrical stimulation studies in rhesus monkeys as a region producing contraversive horizontal saccades (Cohen et al., 1985). More recently, the cMRF's inclusion amongst regionsthat participate in horizontal gaze activity has been supported by a retrograde trans-synaptic tracer study showing that it is multisynaptically connected to the lateral rectus muscle (Ugolini et. al., 2006). Several recording studies have followed the initial cMRF stimulation experiments (Waitzman et al., 1996; 2000; Handel and Glimcher, 1997; Pathmanathan et al., 2006a&b). Most have emphasized a role in the horizontal component of gaze (but see Handel and Glimcher, 1997). Recently, Cromer and Waitzman (2007) found that the saccade-associated bursts of some cMRF neurons have directional tuning, latencies, and temporal encoding of saccade metrics that are similar to saccade-related neurons in the paramedian pontine reticular formation (PPRF). However, the activity patterns in other cMRF neurons more closely resembled neurons in the SC. It is likely that the latter are part of a feedback circuit that modulates gaze-related activity in the SC.

Despite considerable evidence for a role of the primate cMRF in gaze, there are surprisingly few studies that have directly investigated the connections of this structure (Cohen and Büttner-Ennever, 1984). Chen and May (2000) injected biotinylated dextran amine (BDA) into the SC of cynomolgus monkeys, and noted an overlap between retrogradely labeled reticular neurons and anterogradely labeled tectoreticular terminals in a restricted area of the midbrain reticular formation (MRF). They suggested that this area of overlap represents the anatomical correlate of the physiologically defined cMRF. Moreover, there was an extensive relationship between the boutons of labeled tectoreticular axons and labeled reticulotectal cells. This strong reciprocal connection between the SC and cMRF indicates the presence of a feedback loop that presumably modifies the gaze signals generated in the SC. Nevertheless, the targets of this feedback within the SC have received limited investigation (Edwards and de Olmos, 1976; Moschovakis et al., 1988b). The primary objective of the present study was therefore to expand our understanding of these connections by using neuroanatomical tracer methods to define the targets of cMRF input within the SC. Portions of this work have been described previously in abstract form (Zhou et al., 2006).

Materials and Methods

All animal procedures were undertaken in accordance with the animal care and use guidelines of the NIH, including the Principles of Laboratory Care, and with the approval of the University of Mississippi Medical Center IACUC. Six *Macaca fascicularis* monkeys underwent surgeries performed with sterile techniques under isoflurane anesthesia (1–3 %). Animals were preanesthetized with ketamine HCl (10 mg/kg, IM). Atropine sulfate (0.2 mg, IV) was administered to reduce airway secretions. Dexamethasone (0.4 mg, IV) was given to minimize cerebral edema. Core temperature, respiration, heart rate, and blood O_2 saturation, were monitored and maintained within physiological levels. Cortex overlying the midbrain was aspirated to allow direct visualization of the surface of the SC and caudal pole of the pulvinar. Pressure injections were made with a 1.0 μl Hamilton microsyringe attached to a micromanipulator. To avoid the SC, the needle was inserted through the dorsal surface of the pulvinar, with the injection depth adjusted with respect to the SC surface. The coordinates used were based on previous anatomical (Chen and May, 2000) and physiological descriptions (Cohen et al., 1985), and atlas information (Paxinos et al., 2000).

Between 0.1 and 0.2 μl of a 10.0% solution of biotinylated dextran amine (BDA, Molecular Probes) was delivered into the left cMRF along each of 1 or 2 penetrations. The incision was closed and the wound edges were infused with Sensorcaine. Buprenex (0.01 mg/kg, IM) was administered as a postsurgical analgesic.

After a 3 week survival period, animals were sedated with ketamine HCl (10 mg/kg, IM) and deeply anesthetized with sodium pentobarbital (50 mg/kg, IP). They were then perfused transcardially with buffered saline, followed by a fixative containing 1% paraformaldehyde and 1.25–1.5 % glutaradehyde in 0.1 M pH 7.2 phosphate buffer (PB). Frontal sections were cut at 100 μm with a vibratome (Leica VT1000S). At least two rostrocaudal series at 300 μm intervals (i.e., each was a 1 in 3 series) were reacted for BDA. Specifically, the sections were incubated overnight at 4°C in avidin D conjugated to horseradish peroxidase (Vector, 1:5000) in a solution containing 0.05% triton X-100 in 0.1 M, pH 7.2 PB. Sections then were rinsed with 0.1 M, pH 7.2 PB and reacted in a 5.0 % diaminobenzedine (DAB) solution in 0.1 M, pH 7.2 PB containing 0.011% hydrogen peroxide, 0.05% nickel ammonium sulfate and 0.05% cobalt chloride for 10–30 min. BDA-labeled profiles in the SC were charted and drawn with a Nikon Eclipse 80i or Olympus BH2 microscope fitted with a drawing tube. Digital images were made with a Nikon Eclipse E600 photomicroscope outfitted with a Nikon Digital DXM1200F camera, as directed by MetaMorph analysis software. A series of up to 15 Z-axis planes approximately 1 μm apart can be merged by means of the stack arithmetic function of Metamorph. Contrast and brightness were adjusted in Adobe Photoshop to appear comparable to the visualized image.

Boundary determination in the cMRF and SC was based on our previous studies (Chen and May, 2000; May and Porter, 1992; Warren et al., 2008). The medial border of the cMRF is formed by the medial longitudinal fasciculus and the periaqueductal gray, and the lateral border is formed by a dorsoventrally running white matter bundle that includes fibers of the medial lemniscus. Its rostral boundary lies just caudal to the level of the interstitial nucleus of Cajal. At its caudal end, the rostral pole of the inferior colliculus expands within the midbrain leaving the cMRF to occupy an increasingly narrow medial and ventral rim. In terms of the dorsoventral extent of the MRF, it occupies the central half of the region. The MRF dorsal to it lacks the scattered larger cells of the cMRF, and the MRF ventral to it has greater numbers of interspersed fibers.

Results

We observed different projection patterns in the SC that correlated with the location of the cMRF injection site. Two examples are presented to illustrate this point. Monkey A had BDA injections that nearly filled the cMRF, while monkey B had a smaller BDA injection confined to the central part of the cMRF.

Distribution of labeled reticulotectal terminal fields

The extent of the tracer spread from two tracks made in monkey A is illustrated in figure 1A&B. The injection site includes most of cMRF, and is largely confined to the dorsal part of the midbrain reticular formation (MRF), with slight extension into the lateral periaqueductal gray. The lateral and medial locations of these injections can be further appreciated in figure 2A. Anterogradely labeled axon terminals were located bilaterally within the SC, with an ipsilateral predominance (Fig. 1C–H). They were present throughout its rostrocaudal and mediolateral extent. The most prominent terminal fields were evident in the ipsilateral and contralateral intermediate gray layer (SGI), but terminals were also present in the layers beneath SGI and in the periaqueductal gray. In addition, labeled terminals spread dorsally from SGI into stratum opticum (SO), and even extended into the lower region of the superficial gray layer (SGS) on the ipsilateral side. Retrogradely labeled

SC neurons projecting to the cMRF were present, with the vast majority distributed within ipsilateral SGI (Fig. 1C–H). Occasional labeled cells were also present in the ipsilateral intermediate white layer (SAI)(Fig. 1E&F) and deep gray layer (SGP)(Fig. 1D–H), and a few labeled cells were seen in contralateral SGI (Fig. 1D–F).

The BDA injection site for monkey B was confined to the central aspect of the dorsal MRF (Fig. 3A&B) and covered a distinctly smaller area than monkey A's injections (Fig. 2B). Once again, the anterogradely labeled terminals were bilaterally distributed throughout the rostrocaudal and mediolateral extent of the SC, with an ipsilateral predominance (Fig. 3C–H). Labeled terminals were evident in all the ipsilateral layers, and in all layers except SGS, contralaterally. However, the terminals in monkey B were distinctly denser in the upper half of ipsilateral SGI. This difference is shown in figure 2, where the concentration of BDA labeled boutons in the upper (Fig. 2C) and lower (Fig. 2D) portions of SGI can be compared. Differences were also evident in the pattern of retrograde labeling. The vast majority (72 %) of retrogradely labeled neurons were located in the upper half of SGI (Fig. 3C–H) in comparison to the situation in monkey A, where the upper half of SGI contained 56 % of the labeled cells. Labeled tectoreticular neurons were not generally observed contralaterally, or ventral to the ipsilateral SGI. Thus, the upper sublamina of SGI appears to be preferentially labeled following an injection confined to the central portion of the cMRF. (See May and Porter, 1992, for SGI sublaminar definitions.)

The other cases from this study supported the differences seen in monkeys A and B. Figure 4A shows the pattern of terminal and cell label following a cMRF injection in the central part of the nucleus that spread medially to the edge of the periaqueductal gray (Fig. $4A_{1\&2}$). This injection also included the MRF dorsal and ventral to the cMRF. As with monkey A, labeled terminals and cells were distributed evenly throughout SGI, without regard to the sublaminae (Fig. $4A_{3–7}$). The presence of labeling in the superficial layers (Fig. $4A_{5–7}$) is presumably due to spread of tracer up the needle track into the pretectum and pulvinar. In contrast, figure 4B shows a case that was similar to monkey B. In this case, the small injection site was confined to the lateral cMRF and MRF dorsal to it (Fig. $4B_{1\&2}$). The terminal labeling was generally lighter than in monkey B, but the greater density of terminals in upper, as opposed to lower, SGI was still evident (Fig. $4B_{3–7}$). Clearly, there were also more labeled tectoreticular neurons in the upper sublamina (Fig. $4B_{3–7}$). Some tracer entered the needle track, and resulted in cell labeling in the superficial layers (Fig. $4B_{5\&6}$). The final 2 monkeys both had patterns of anterograde and retrograde labeling similar tomonkey A's. One had a double injection like Monkey A's, while the second was similar to that shown in Fig. 4A, but in both cases the injection sites extended further ventrally beyond the MRF's boundaries.

Relationship between reticulotectal terminals and tectoreticular neurons

Figure 5 shows the labeling observed in SGI of monkey A. Well labeled multipolar neurons were present in both upper (Fig. 5A&B) and lower (Fig. 5C&D) SGI. Labeled axons were also visible. They displayed numerous *en passant* boutons of various sizes. Most of the labeled boutons were distributed within the neuropil, where their tectal targets could not be identified. Nevertheless, in some cases, close associations (arrowheads) between the boutons of the BDA labeled axons and BDA labeled tectoreticular neurons were noted (Fig 5A–D), with dendritic appositions most frequently observed.

The range of the morphology of the BDA labeled neurons and axons for monkey A is further illustrated in figure 6. Retrogradely transported BDA filled the primary dendrites and extended, in some cases, as far as the tertiary dendrites. The neurons located in upper (Fig. 6A–E), and lower SGI (Fig. 6G–N) all displayed a similar organization. Most were medium or large multipolar neurons (25–40 μm long axis). Labeled reticulotectal axonal arbors

displayed boutons that lay in close association (arrowheads) with the somata (Fig. 6B&I) and dendrites (Fig. 6A–N) of the labeled cells.

For comparison, photomicrographs of labeled neurons from monkey B are shown in figure 7. Neurons in upper SGI (Fig. 7A–C) were usually well labeled, with the dark reaction product extending far into their dendritic trees. By contrast, those in ventral SGI were often substantially more lightly labeled (Fig. 7D). No obvious morphological differences were discerned between neurons in the two sublaminae. However, the presence of light label in the lower SGI neurons suggests that few terminals from these cells were distributed within the core of the cMRF injection. In both sublaminae, close associations (arrowheads) between these labeled neurons and the boutons of the BDA labeled axons were present (Fig. 7A–D). These close associations were observed on both the somata (Fig. 7B–D) and dendrites (Fig. 7A–D) of the tectoreticular neurons.

Further examples of the labeling for monkey B are illustrated in figure 8. Most of the BDA labeled neurons were located in the upper sublamina of SGI (Fig. 8A–F), with only a few examples available from the lower sublamina (Fig. 8G–I). Nevertheless, the morphology of the cells in the two sublaminae was similar. Furthermore, the boutons of labeled axons displayed close associations (arrowheads) with the somata (Fig. 8A,F,H,I) and dendrites (Fig. 8B–I) of most of the labeled neurons found in both upper (Fig. 8A–F) and lower (Fig. 8G–I) SGI.

Discussion

The results of this study indicate that the cMRF projects heavily upon the SC. Reticulotectal terminal arbors were distributed bilaterally, with an ipsilateral predominance, primarily in SGI. The SC cells that project upon the cMRF were also found primarily within the ipsilateral SGI. The close associations between reticulotectal boutons and tectoreticular cells suggest that one target of the cMRF projections is the population of collicular neurons that projects back to the cMRF. This bidirectional configuration indicates a feedback loop connects cMRF neurons projecting to the SC and collicular output cells, whose collaterals terminate in the cMRF. Finally, we found that differences in the site of the cMRF injection resulted in differences in the pattern of SC labeling, suggesting the sublaminae of SGI are differentially connected with the lateral and medial portions of the cMRF.

Relationship to previous findings

The presence of anterogradely labeled reticulotectal terminals within the SC is consistent with the findings of retrograde tracer studies that have revealed labeled neurons in the MRF after injections of the SC (Edwards et al., 1979; Chen and May, 2000; May et al., 2002; May, 2006; Warren et al., 2008). However, to the best of our knowledge, this is the first anterograde tracer study demonstrating the terminal distribution pattern of this projection in monkeys. A pattern like that shown in the present study was observed following injections of the cat cuneiform nucleus, a structure that would include the cMRF as defined here (Edwards and de Olmos, 1976; see Chen and May, 2000 and Warren et al., 2008). Specifically, labeled terminals were found in cat SGI and SGP, with an ipsilateral predominance. This terminal distribution pattern also agrees with that revealed with intra-axonal staining by Moschovakis and colleagues (1988b). They stained 5 long-lead burst neurons in the MRF of squirrel monkeys whose axons terminated in the SGI. Some cells only terminated ipsilaterally, but the main axon of others crossed the intertectal commissure to terminate contralaterally. As the present results are generally consistent with the laterality and laminar organization seen with intracellular staining, we feel it is unlikely that they are due to uptake by fibers of passage or spread of tracer outside the borders of the target

structure. Still, it is possible that some BDA labeled terminals were contributed by local axon collaterals of tectoreticular cells (Moschovakis et al., 1988a).

The retrogradely labeled tectoreticular neurons observed following cMRF injections were located primarily within ipsilateral SGI, with smaller numbers in SAI and SGP. This is in substantial agreement with a previous investigation by Cohen and Büttner-Ennever (1984). They used physiologically localized injections to demonstrate that dorsal cMRF sites that produce small saccades receive input from the rostral SC, and ventral sites that produce large saccades receive input from the caudal SC. The dorsoventral extent of our injections did not allow us to test this point. No differences were seen with respect to SC gaze topography with changes in the rostrocaudal or mediolateral position of our injections, but ordered changes in saccade vector have not been reported in the cMRF along these planes (Cohen et al., 1985; Waitzman et al., 1996).

The SC exhibits two major descending projections, the ipsilateral tectopontine-tectobulbar tract and the crossed tectobulbospinal tract (or predorsal bundle). The current retrograde data can not, in and of themselves, differentiate whether the labeled cells belong to the ipsilateral or contralateral descending pathway. However, intracellular studies in cat and monkey indicate that axons in the crossed projection, but not the ipsilateral one, provide extensive collateral terminations within the ipsilateral MRF (Grantyn and Grantyn, 1982; Moschovakis et al., 1988a&b). Thus, we expect that most of the BDA labeled neurons observed in the present study represent cells whose axons project in the predorsal bundle.

The cMRF feedback loop

The cMRF is not only a major target for SC output (Harting, 1977), but it also provides reciprocal reticulotectal projections that feed back upon the SC (Moschovakis et al., 1988b; Chen and May, 2000; May et al., 2002; Warren et al., 2008). The fact that cMRF reticulotectal neurons often receive multiple close associations from tectoreticular boutons suggests the activity of these cells is dominated by collicular input (Chen and May, 2000; May et al., 2002). Indeed, Moschovakis and colleagues (1988b) reported that the saccade-related activity recorded in cMRF reticulotectal neurons was virtually indistinguishable from that recorded in collicular long lead burst neurons with respect to onset or peak firing. Presumably such feedback neurons fall into the category in which firing rate encodes saccade amplitude (Cromer and Waitzman, 2006).

The present study provides insights into the prospective SC targets of this feedback signal. Reticulotectal terminals were concentrated in the SC layers ventral to SGS, which contain the cells of origin for both the ipsilateral and contralateral descending pathways (May, 2006). The majority of BDA labeled boutons were distributed within the neuropil. Thus, it is likely that they target other populations of SC neurons, such as those projecting ipsilaterally, or that they influence interneuron populations within these layers, many of which are GABAergic (Mize, 1996) and have connections with SC output neurons (Fuentes-Sanatmaria et al., 2007). In particular, the present study demonstrated the presence of close associations between reticulotectal boutons and retrogradely labeled tectoreticular neurons. Although ultrastructural evidence will be required to unequivocally establish that these represent synaptic contacts, the present data provide suggestive evidence for such a connection. As these labeled SC neurons probably give rise to the predorsal bundle, it appears that the cells providing the dominant input to cMRF reticulotectal neurons, are among the targets of the cMRF feedback signal, producing a closed feedback loop at the neuronal level. This may be a widespread characteristic, as similar neuronal connections have been observed in goldfish (Pérez- Pérez et al., 2003; Luque et al., 2005). The density of feedback input onto predorsal bundle neurons suggests it would modulate, but not dominate, the burst of saccade-related activity seen in these SC neurons (Moschovakis et al., 1988b;

Munoz et al., 1991). Indeed, it has been hypothesized that feedback by the cMRF could contribute to maintaining saccade accuracy (Cromer and Waitzman, 2006), as inactivation of the cMRF produces hypermetric saccades in monkeys (Waitzman et al., 2000), and at least a portion of the cat MRF reticulotectal population is GABA positive (Appell and Behan, 1990).

One of the striking features of the results is the bilateral distribution of reticulotectal terminals throughout the SC. Given that the two sides of the SC act as antagonists for the horizontal component of gaze changes (Behan, 1985; Munoz and Istevan, 1998; Olivier et al., 1998; Takahashi et al., 2005), the function of this bilateral cMRF projection is not immediately clear. Perhaps one side of this bilateral projection selectively targets interneurons to reverse the polarity of its effects.

Gaze channels

In the present study, BDA injections that did not involve the medial cMRF labeled cells and terminals that were preferentially concentrated in upper SGI. In contrast, when injections included the medial cMRF, there was no significant distribution difference between upper and lower SGI. This suggests that medial aspects of cMRF are connected to lower SGI and lateral aspects of cMRF are connected to upper SGI. This is noteworthy because injections of the spinal cord in the cat and monkey retrogradely label reticulospinal neurons that are largely confined to the medial region of the cMRF (Castiglioni et al., 1978; Robinson et al., 1994; Warren et al., 2008). Furthermore, a study of primate SC projections by May and Porter (1992) showed that the lower sublamina of SGI is preferentially connected to the spinal cord, whereas the upper sublamina is preferentially connected to the PPRF. This sublaminar difference is supported by an electrical stimulation study, which showed that the propensity for inducing head movements increases with SC penetration depth (Cowie and Robinson, 1994). Thus, we postulate that the cMRF may contain subregions that provide individual feedback loops for the upper, more eye-related sublamina of SGI, and lower, more head-related sublamina of SGI (Fig. 9). Such independent manipulation would seem reasonable in light of the capacity shown by primates to regulate the presence and extent of a gaze-related head movement (Fuller, 1992; Goosens and Van Opstal, 1997; Stahl, 2001), and the fact that the SC contains several neuronal populations: those that respond before eye movements, before head movements and before gaze changes involving both the eyes and head (Walton et al., 2007).

Based on the retrograde labeling pattern, the lateral (more eye-related) and medial (more head-related) portions of the cMRF may be targeted by discrete inputs from the upper and lower sublaminae of SGI (Fig. 9). Presumably, these inputs also influence the descending pathways originating in the cMRF that modulate eye and head movements. Thus, lower SGI is positioned to influence the activity of cMRF reticulospinal neurons through its projections to medial cMRF. Unlike the crossed tectospinal projection, the cMRF descending projection targets the ipsilateral spinal cord. It has been suggested (Warren et al., 2008) that this projection is responsible for the inhibition of antagonist neck muscles observed during head gaze movements or the excitation of antagonist neck muscles that sometimes halts swift targeted head movements (Roucoux et al., 1989;Corneil et al., 2001).

Acknowledgments

The authors are grateful to Dr. Olga Golanov for her excellent histological work and help in the production of the figures. We are indebted to Dr. John McHaffie for his thoughtful comments on an earlier draft of this work.

List of Figure Abbreviations

III	oculomotor nucleus
BC	brachium conjunctivum
BDA	biotinylated dextran amine
cMRF	central mesencephalic reticular formation
IC	inferior colliculus
lSGI	lower SGI
MD	medial dorsal nucleus
MG	medial geniculate
nPC	nucleus of posterior commissure
PAG	periaqueductal gray
PN	pontine nucleus
PRF	pontine reticular formation
Pt	pretectum
Pul	pulvinar
SAI	intermediate white layer
SGI	intermediate gray layer
SGP	deep gray layer
SGS	superficial gray layer
SO	stratum opticum
uSGI	upper SGI

References

Appell PP, Behan M. Sources of subcortical GABAergic projections to the superior colliculus in the cat. J Comp Neurol 1990;302:143–158. [PubMed: 2086611]

Behan M. An EM-autoradiographic and EM-HRP study of the commissural projection of the superior colliculus in the cat. J Comp Neurol 1985;234:105–116. [PubMed: 3980783]

Castiglioni AJ, Gallaway MC, Coulter JD. Spinal projections from the midbrain in monkey. J Comp Neurol 1978;178:329–346. [PubMed: 415074]

Chen B, May PJ. The feedback circuit connecting the superior colliculus and central mesencephalic reticular formation: a direct morphological demonstration. Exp Brain Res 2000;131:10–21. [PubMed: 10759167]

Cohen B, Büttner-Ennever JA. Projections from the superior colliculus to a region of the central mesencephalic reticular formation (cMRF) associated with horizontal saccadic eye movements. Exp Brain Res 1984;57:167–176. [PubMed: 6519224]

Cohen B, Matsuo V, Fradin J, Raphan T. Horizontal saccades induced by stimulation of the central mesencephalic reticular formation. Exp Brain Res 1985;57:605–616. [PubMed: 3979501]

Corneil BD, Olivier E, Richmond FJ, Loeb GE, Munoz DP. Neck muscles in the rhesus monkey. II. Electromyographic patterns of activation underlying postures and movements. J Neurophysiol 2001;86:1729–1749. [PubMed: 11600635]

Cowie RJ, Robinson D. Subcortical contributions to head movements in macaques. 1. Contrasting effects of electrical stimulation of a medial pontomedullary region and the superior colliculus. J Neurophysiol 1994;72:2648–2664. [PubMed: 7897481]

Cromer JA, Waitzman DM. Neurones associated with saccade metrics in the monkey central mesencephalic reticular formation. J Physiol 2006;570:507–523. [PubMed: 16308353]

Cromer JA, Waitzman. Comparison of saccade-associated neuronal activity in the primate central mesencephalic and paramedian pontine reticular formations. J Neurophysiol 2007;98:835–850. [PubMed: 17537904]

Edwards SB, de Olmos JS. Autoradiographic studies of the projections of the midbrain reticular formation: ascending projection of nucleus cuneiformis. J Comp Neurol 1976;165:417–432. [PubMed: 1262539]

Edwards SB, Ginsburgh CL, Henkel CK, Stein BE. Sources of subcortical projections to the superior colliculus in the cat. J Comp Neurol 1979;184:309–329. [PubMed: 762286]

Freedman EG, Sparks DL. Activity of cells in the deeper layers of the superior colliculus of the rhesus monkey: evidence for a gaze displacement command. J Neurophysiol 1997;78:1669–1690. [PubMed: 9310452]

Fuentes-Santamaria V, Alvarado JC, Stein BE, McHaffie JG. Cortex contacts both output neurons and nitrergic interneurons in the superior colliculus: Direct and indirect routes for multisensory integration. Cereb Cortex. 2007 (In Press).

Fuller JH. Head movement propensity. Exp Brain Res 1992;92:152–164. [PubMed: 1486950]

Goosens HH, Van Opstal AJ. Human eye-head coordination in two dimensions under different sensorimotor conditions. Exp Brain Res 1997;114:542–560. [PubMed: 9187290]

Grantyn A, Grantyn R. Axonal patterns and sites of termination of cat superior colliculus neurons projecting in the tecto-bulbo-spinal tract. Exp Brain Res 1982;46:243–256. [PubMed: 7095033]

Handel A, Glimcher PW. Response properties of saccade-related burst neurons in the central mesencephalic reticular formation. J Neurophysiol 1997;78:2164–2175. [PubMed: 9325383]

Harting JK. Descending pathways from the superior colliculus: an autoradiographic analysis in the rhesus monkey (*Macaca mulatta*). J Comp Neurol 1977;173:583–612. [PubMed: 404340]

Luque MA, Pérez- Pérez MP, Herrero L, Torres B. Involvement of the optic tectum and mesencephalic reticular formation in the generation of saccadic eye movements in goldfish. Brain Res Rev 2005;49:388–397. [PubMed: 16111565]

May PJ. The mammalian superior colliculus: laminar structure and connections. Prog Brain Res 2006;151:321–378. [PubMed: 16221594]

May PJ, Porter JD. The laminar distribution of macaque tectobulbar and tectospinal neurons. Vis Neurosci 1992;8:257–276. [PubMed: 1372175]

May PJ, Warren S, Chen B, Richmond FJR, Olivier E. Midbrain reticular formation circuitry subserving gaze in the cat. Ann NY Acad Sci 2002;956:405–408. [PubMed: 11960826]

Mize RR. Neurochemical microcircuitry underlying visual and oculomotor function in the cat superior colliculus. Prog Brain Res 1996;112:35–55. [PubMed: 8979819]

Moschovakis AK, Karabelas AB, Highstein SM. Structure-function relationships on the primate superior colliculus. I. Morphological classification of efferent neurons. J Neurophysiol 1988a; 60:232–262. [PubMed: 3404219]

Moschovakis AK, Karabelas AB, Highstein SM. Structure-function relationships in the primate superior colliculus. II. Morphological identity of presaccadic neurons. J Neurophysiol 1988b; 60:263–298. [PubMed: 3404220]

Moschovakis AK, Kitama T, Dalzios Y, Petit J, Brandi AM, Grantyn AA. An anatomical substrate for the spatiotemporal transformation. J Neurosci 1998;18:10219–10229. [PubMed: 9822775]

Munoz DP, Guitton D, Pelisson D. Control of orienting gaze shifts by the tectoreticulospinal system in the head-free cat. III. Spatiotemporal characteristics of phasic motor discharges. J Neurophysiol 1991;66:1642–1666. [PubMed: 1765799]

Munoz DP, Istevan PJ. Lateral inhibitory interactions in the intermediate layers of the monkey superior colliculus. J Neurophysiol 1998;79:1193–1209. [PubMed: 9497401]

Olivier E, Porter JD, May PJ. Comparison of the distribution and somatodendritic morphology of tectotectal neurons in the cat and monkey. Vis Neurosci 1998;15:903–922. [PubMed: 9764533]

Pathmanathan JS, Presnell R, Cromer JA, Cullen KE, Waitzman DM. Spatial characteristics of neurons in the central mesencephalic reticular formation (cMRF) of head-unrestrained monkeys. Exp Brain Res 2006a;168:455–470. [PubMed: 16292575]

Pathmanathan JS, Cromer JA, Cullen KE, Waitzman DM. Temporal characteristics of neurons in the central mesencephalic reticular formation of head unrestrained monkeys. Exp Brain Res 2006b; 168:471–492. [PubMed: 16292574]

Paxinos, G.; Huang, X-F.; Toga, AW. The Rhesus Monkey Brain in Stereotaxic Coordinates. Academic Press; San Diego: 2000.

Pérez- Pérez MP, Luque MA, Herrero L, Nunez-Abades PA, Torres B. Connectivity of the goldfish optic tectum with the mesencephalic and rhomencephalic reticular formation. Exp Brain Res 2003;151:123–135. [PubMed: 12748838]

Robinson FR, Phillips JO, Fuchs AF. Coordination of gaze shifts in primates: brainstem inputs to neck and extraocular motoneuron pools. J Comp Neurol 1994;346:43–62. [PubMed: 7962711]

Roucoux A, Crommelinck M, Decostre MF. Neck muscle activity in eye-head coordinated movements. Prog Brain Res 1989;80:351–62. [PubMed: 2634276]

Stahl JS. Eye-head coordination and the variation of eye-movement accuracy with orbital eccentricity. Exp Brain Res 2001;36:200–210. [PubMed: 11206282]

Stryker MP, Schiller PH. Eye and head movements evoked by electrical stimulation of monkey superior colliculus. Exp Brain Res 1975;23:103–112. [PubMed: 1149845]

Takahashi M, Sugiuchi Y, Izawa Y, Shinoda Y. Commissural excitation and inhibition by the superior colliculus in tectoreticular neurons projecting to omnipause neuron and inhibitory burst neuron regions. J Neurophysiol 2005;94:1707–1726. [PubMed: 16105954]

Ugolini G, Klam F, Dans MD, Dubayle D, Brandi AM, Büttner-Ennever J, Graf W. Horizontal eye movement networks in primates as revealed by retrograde transneuronal transfer of rabies virus: differences in monosynaptic input to “slow” and “fast” abducens motoneurons. J Comp Neurol 2006;498:762–785. [PubMed: 16927266]

Waitzman DM, Silakov VL, Cohen B. Central mesencephalic reticular formation (cMRF) neurons discharging before and during eye movements. J Neurophysiol 1996;75:1546–1572. [PubMed: 8727396]

Waitzman DM, Silakov VL, DePalma-Bowles S, Ayers AS. Effects of reversible inactivation of the primate mesencephalic reticular formation. I. Hypermetric goal-directed saccades. J Neurophysiol 2000;83:2260–2284. [PubMed: 10758133]

Walton MMG, Bechara B, Gandhi NJ. Role of primate superior colliculus in the control of head movements. J Neurophys 2007;98:2022–2037.

Warren S, Waitzman DM, May PJ. Anatomical evidence for interconnections between the central mesencephalic reticular formation and cervical spinal cord in the cat and macaque. Anat Rec 2008;291:141–160.

Wurtz RH, Goldberg ME. Activity of superior colliculus in behaving monkey. 3. Cells discharging before eye movements. J Neurophysiol 1972;35:575–586. [PubMed: 4624741]

Zhou L, Warren S, May PJ. Projection of the central mesencephalic reticular formation in the macaque. Soc Neurosci Abst 2006;32:139.1.

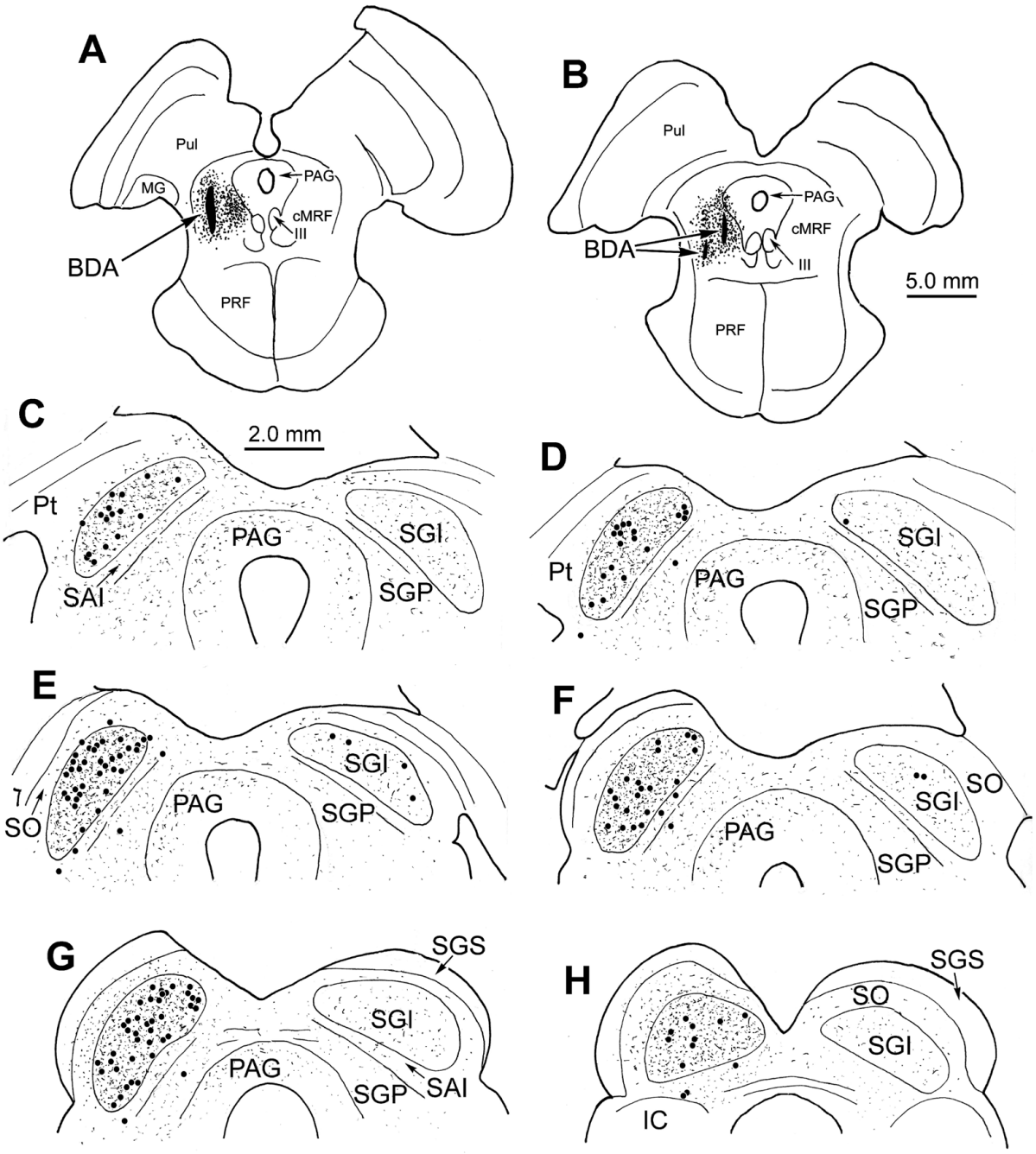

Figure 1.

Distribution of labeled reticulotectal terminal fields and tectoreticular neurons in monkey A. BDA injections nearly filled the cMRF (A&B). Anterogradely labeled axon terminals (stipple) were found in the SC bilaterally, with an ipsilateral predominance (C–H). Retrogradely labeled tectoreticular neurons (dots) were most common in ipsilateral SGI (C–H). The interval between adjacent illustrated levels is 600 μm.

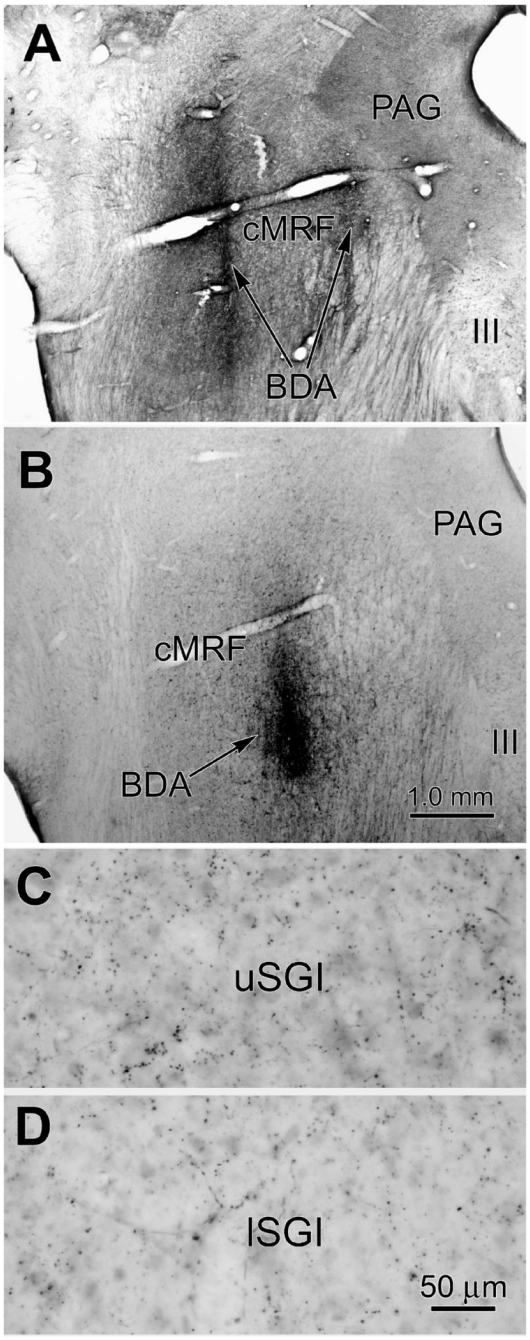

Figure 2.
BDA injection sites and terminal label. Monkey A (see Fig. 1) had a large injection produced by two separate tracks (A), while monkey B (see Fig. 3) had a single small injection in the central part of the cMRF (B). There is a greater terminal density in upper SGI (C) compared to lower SGI (D) following the monkey B injection.

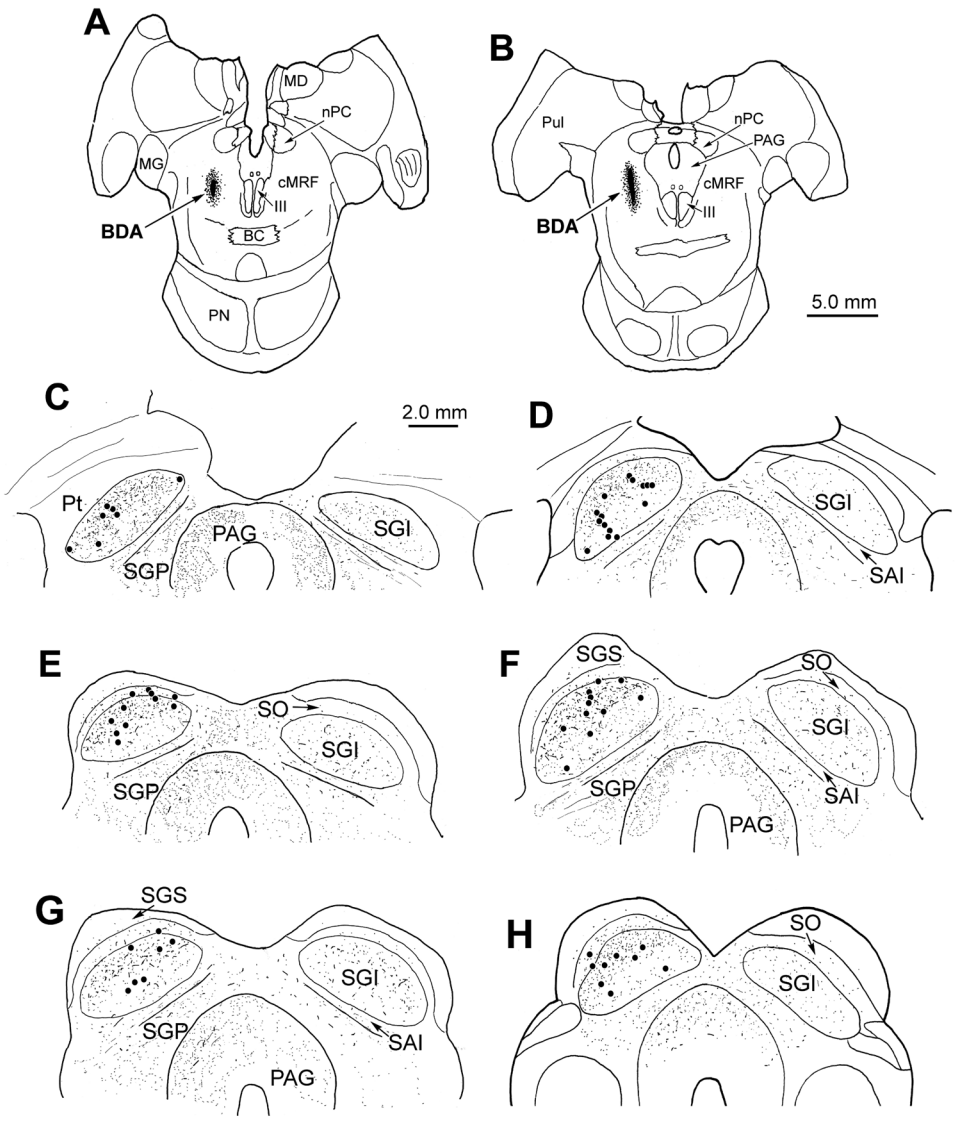

Figure 3.

Distribution of labeled reticulotectal terminal fields and tectoreticular neurons following an injection in the central portion of the cMRF in monkey B (A&B). Anterogradely labeled axon terminals (stipple) were present bilaterally within the intermediate and deep layers of the SC (C–H). However, these terminals were concentrated in the upper half of ipsilateral SGI. Similarly, nearly all of the retrogradely labeled tectoreticular neurons (dots) were observed in the upper sublamina of ipsilateral SGI (C–H). The interval between adjacent illustrated levels is 600 μm.

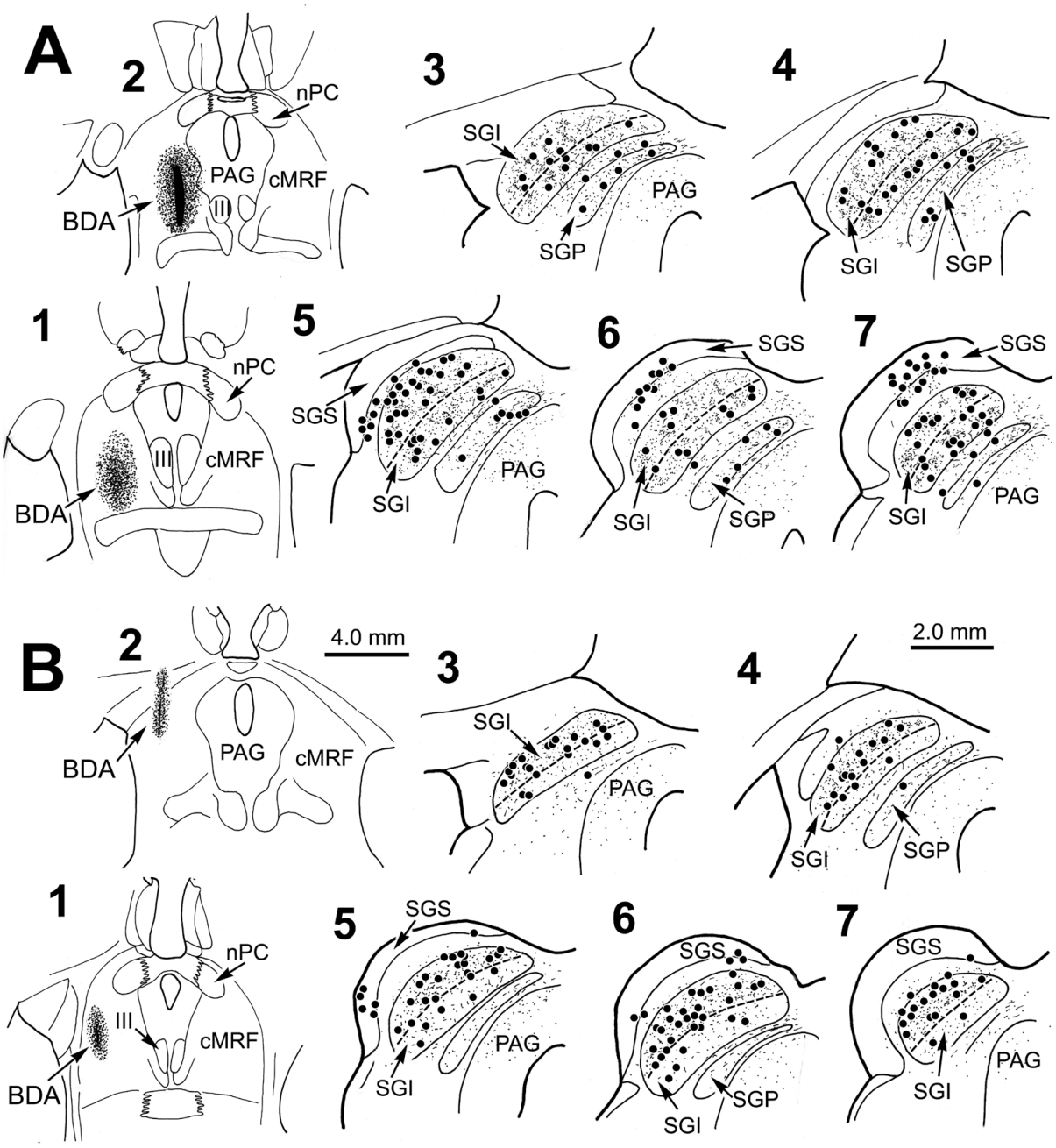

Figure 4.

Distribution of labeled reticulotectal terminal fields and tectoreticular neurons in two additional cases. Following an injection of the central and medial region of the MRF ($A_{1\&2}$) labeled cells (dots) and terminals (stipple) were found throughout SGI, and to a lesser extent in SGP ($A_{3–7}$). Following an injection in the lateral portion of the MRF ($B_{1\&2}$) labeled cells (dots) and terminals (stipple) were much more common in the upper sublamina of SGI. Dashed line indicates the border between upper and lower SGI. The interval between adjacent illustrated levels is 600 μm.

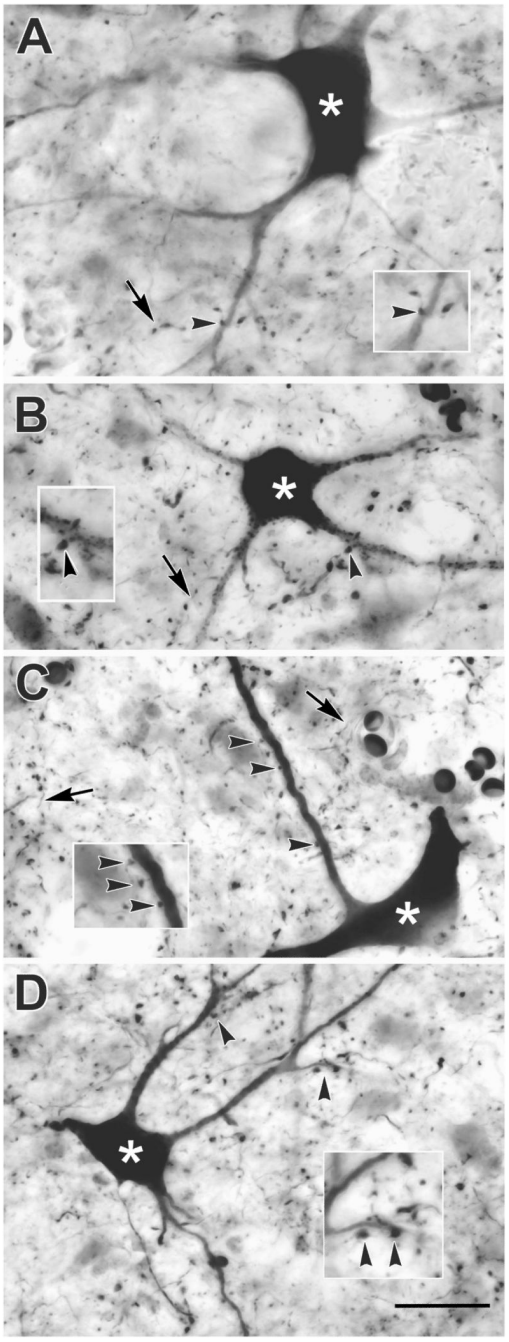

Figure 5.
Photomicrographs of anterogradely labeled reticulotectal axon arbors (arrows) and retrogradely labeled tectoreticular neurons (asterisks) in monkey A. Examples from the upper (A&B) and lower (C&D) sublaminae of SGI are shown. Close associations (arrowheads) were present between the boutons of labeled axons and the dendrites of tectoreticular neurons are shown at higher magnification in inserts. Scale = 25 μm, 40 μm for inserts.

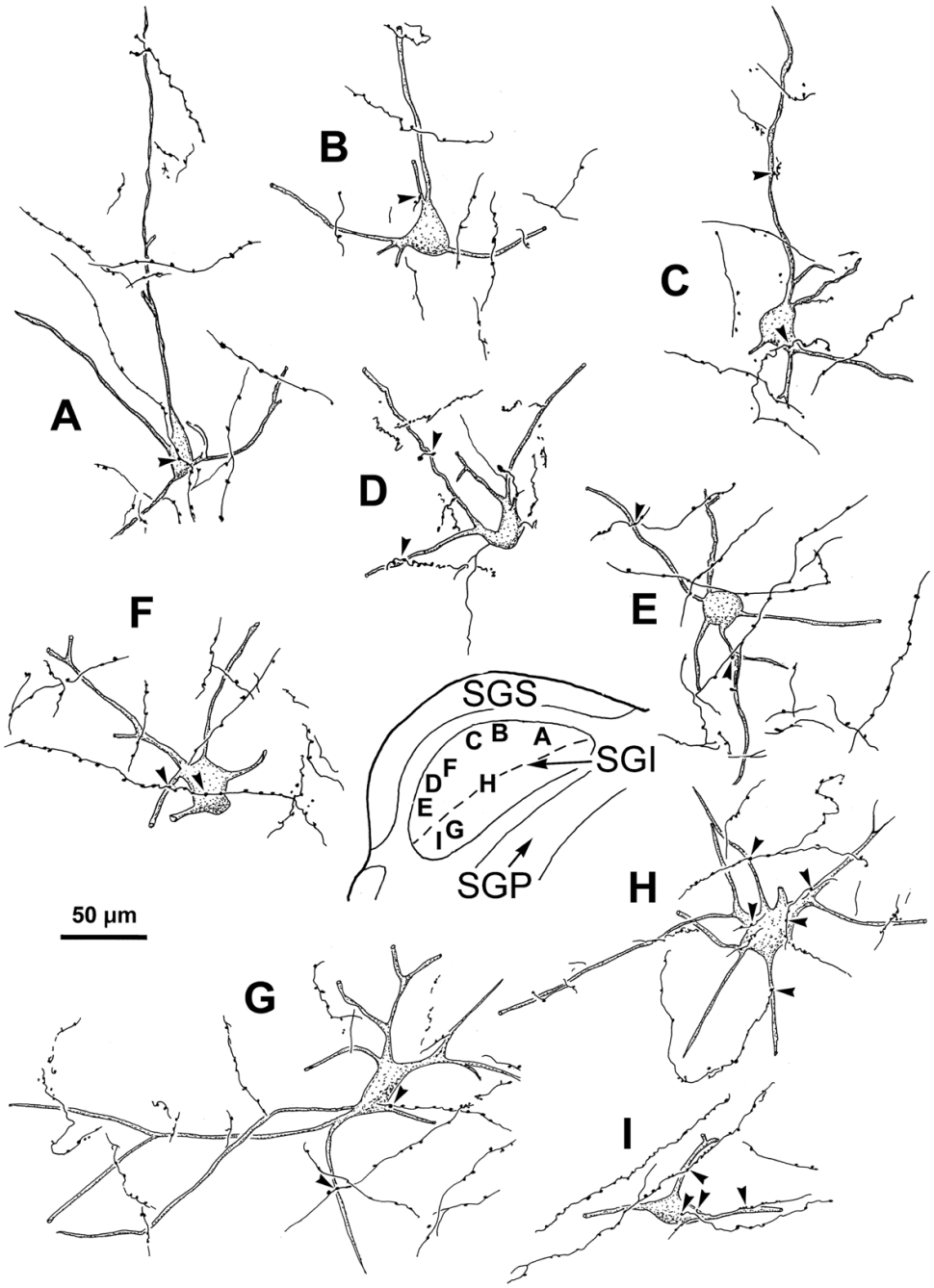

Figure 6.

Labeled tectoreticular neurons and associated reticulotectal axons from monkey A. As shown in the inset, labeled neurons were located in SO (F), the upper sublamina of SGI (A–E) and the lower sublamina of SGI (G–N). Dashed line indicates border between upper and lower SGI. Reticulotectal axonal arbors from the cMRF injection are also illustrated. In some cases, labeled axons displayed boutons that had close associations (arrowheads) with the somata (B & I) and dendrites (A–N) of these cells.

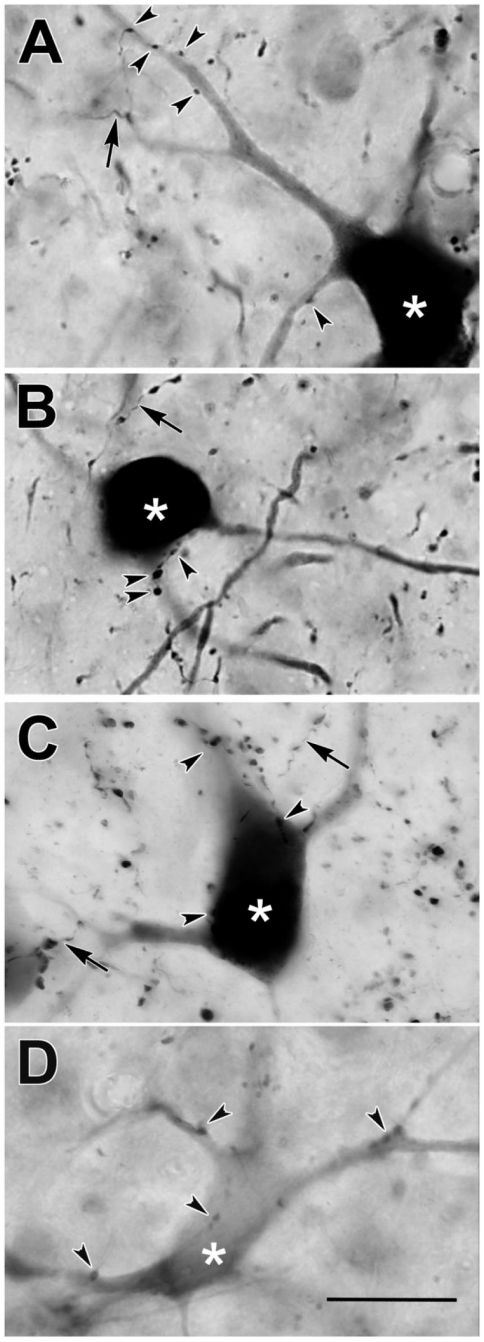

Figure 7.
Photomicrographs of retrogradely labeled tectoreticular neurons (asterisks) and anterogradely labeled reticulotectal axonal arbors (arrows) in monkey B. The labeled neurons located in the upper sublamina of SGI (A–C) were often well labeled with BDA, while examples from the lower sublamina of the SGI (D) were generally much more lightly labeled. Close associations (arrowheads) were present between some reticulotectal boutons and tectoreticular neurons in both sublamina (A–D). Scale = 25 μm.

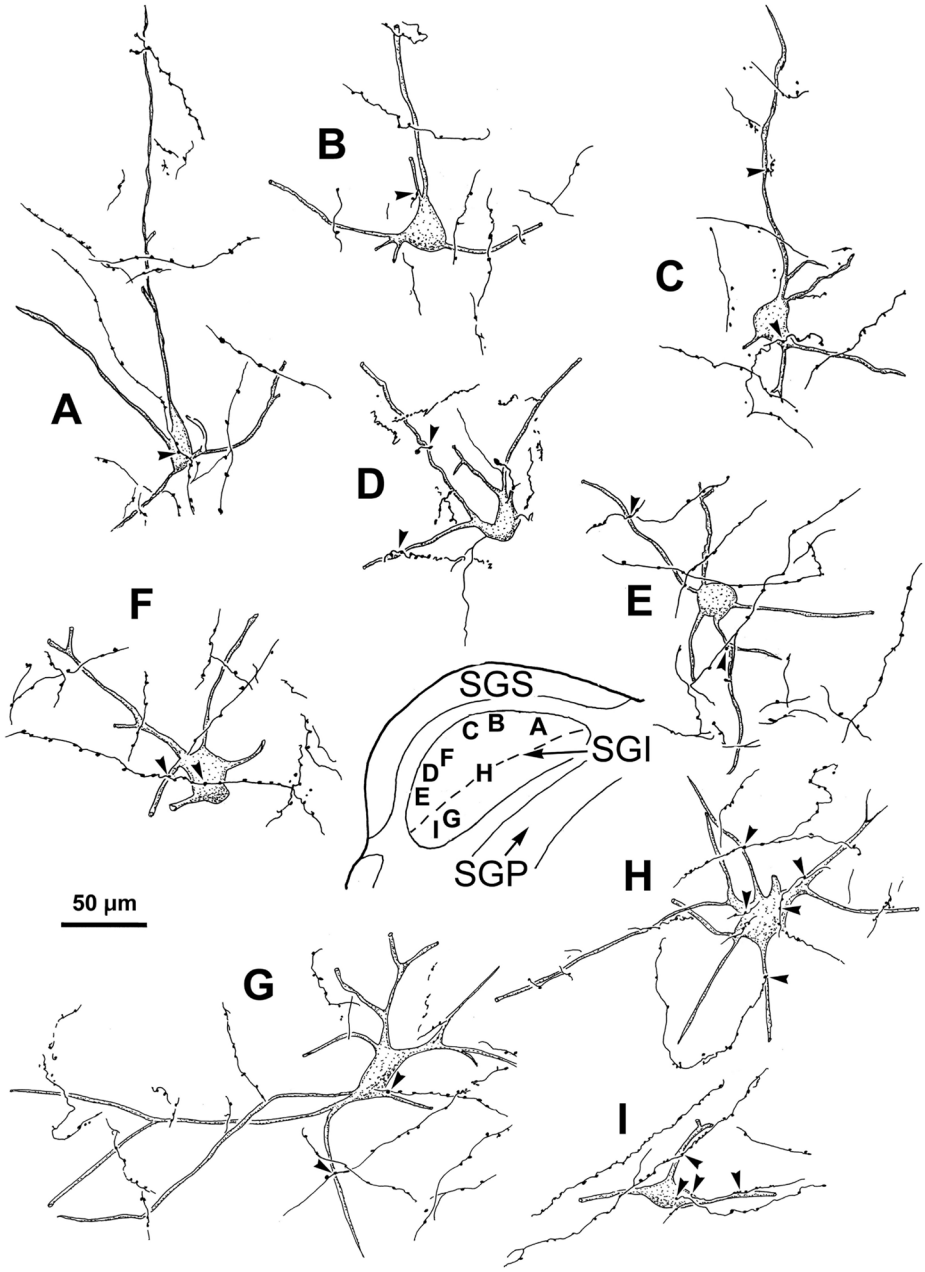

Figure 8.

Labeled tectoreticular neurons and associated reticulotectal axonal arbors from monkey B. As shown in the inset, labeled neurons were mainly located in the upper sublamina of SGI (A–F,H), with only a few found in the lower sublamina (G&I). Dashed line indicates border between upper and lower SGI. In both sublaminae, labeled axons displayed boutons which had close associations (arrowheads) with the somata (A,F,H&I) and dendrites (B–I) of these cells.

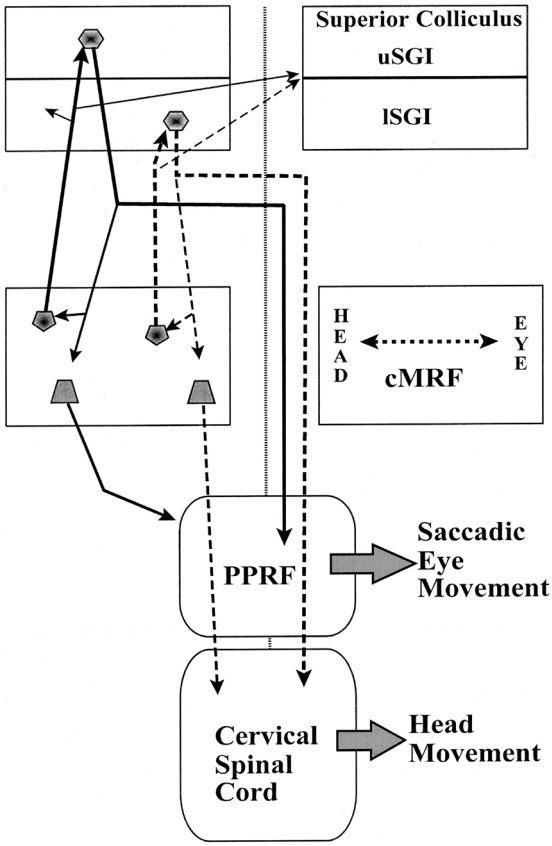

Figure 9.

Summary diagram indicating the proposed relationship between the cMRF and gaze control centers. The eye control channel (continuous lines) begins in the SC's upper sublamina of SGI (uSGI), which sends axons to lateral cMRF, ipsilaterally, and the PPRF, contralaterally. We have shown that the lateral cMRF projects more heavily upon uSGI, and also projects to the PPRF (unpublished data). The head control channel (dashed lines) begins in the lower sublamina of SGI (lSGI), which sends axons to the medial cMRF, ipsilaterally, and cervical spinal cord, contralaterally. The medial cMRF projects more heavily upon lSGI, and also projects to the ipsilateral cervical spinal cord. The present data do not reveal whether the tectal projections directly contact reticuloreticular and reticulospinal neurons. There does not appear to be any sublaminar preference for the crossed pathway.